Table IV. Bimolecular Rate Constants for the Radical Recombination of $Mn(CO)_4L\cdot$, k_r, and Recombination of $Mn_2(CO)_7L_2$ with CO, k', in Hexane and Perfluorohexane at 25 °C

L	solvent	k_r, M^{-1} s^{-1} ^{a}	k', M^{-1} s^{-1} ^{a}
CO	C_6H_{14}	9×10^8	2.9×10^5
CO	C_6F_{14}	1×10^9	3.2×10^5
P(i-Bu)$_3$	C_6H_{14}	2×10^7	2.3×10^3
P(i-Bu)$_3$	C_6F_{14}	2×10^7	4.5×10^3

^{a} ±5%.

be taken to be noninteracting with the $Cr(CO)_5$ intermediate, the rate of recombination with CO approaches the diffusion-controlled limit, as do the recombination rates observed for such weak nucleophiles as N_2, $Cr(CO)_6$, and cyclohexane. These facts are of interest in considering the significance of the measured rate of recombination of $Mn_2(CO)_7L_2$ with CO.

Flash photolysis experiments on $Mn_2(CO)_8L_2$ (L = CO, P(i-Bu)$_3$) in perfluorohexane under a CO atmosphere were conducted to determine the magnitude of the solvent effect. Absorptions were observed in the electronic spectral regions associated with the radical and the unsaturated dimer. The transients decayed as expected following second- and first-order rate laws, respectively. Rate constants measured for radical recombination and unsaturated dimer recombination with CO in hexane and perfluorohexane are organized in Table IV. Radical recombination rates are independent of solvent. Since the rate constants approach a diffusion-controlled limit, the only expected dependence might arise from relatively minor viscosity differences. The rate constants for recombination of $Mn_2(CO)_7L_2$ with CO are also essentially unchanged by the nature of the solvent. Neither intermediate shows the factor of 10^3 differential in the rate constants between alkane and perfluoroalkane solvents observed for $Cr(CO)_5$. Furthermore, neither intermediate has a recombination rate that approaches a diffusion-controlled limit in perfluorohexane. We conclude that hexane molecules are not involved in stabilization of the dimer intermediate. However, there must be some other mode of stabilization of the intermediate; if there were not, it would display a diffusion-limited rate of reaction with CO in perfluoroalkane.

Hepp and Wrighton[12a] recently reported that, following photolysis of $Mn_2(CO)_{10}$ in a cyclohexane matrix, the low-temperature IR spectrum exhibits a band at 1760 cm^{-1}. The intermediate in the matrix was proposed to contain a bridging CO (I). Church et al. have also assigned this absorption, seen

I   II
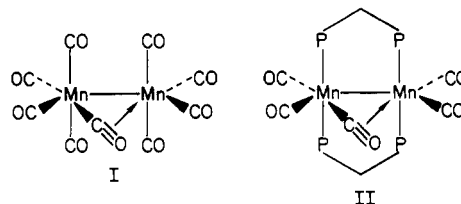
as a transient in the time-resolved IR spectrum, to a bridging species.[12b] The proposed structure of the intermediate is based on the crystal structure of $Mn_2(CO)_5(dppm)_2$ (dppm = 1,2-bis(diphenylphosphino)methane) (II).[22] The bridging CO is apparently not present in 2-methyltetrahydrofuran, a donor solvent. Similar low-temperature matrix experiments yield the same results for $Cp_2Mo_2(CO)_6$.[23]

Our results indicate that the $Mn_2(CO)_7L_2$ intermediates in solution contain an analogous bridge. Through a bridging CO interaction at the coordinatively unsaturated metal center, bringing the electron count at each metal to 18, stabilization by interaction with solvent molecules is precluded. The present results show that the semibridging CO structure is formed rapidly in solution, i.e. on a short time scale with respect to CO recombination, consistent with the time-resolved IR results.[12b]

(22) Commons, C. J.; Hoskins, B. F. *Aust. J. Chem.* **1975**, *28*, 1663.
(23) Hooker, R. H.; Mahmoud, K. A.; Rest, A. J. *J. Organomet. Chem.* **1983**, *254*, C25.

Contribution from the Department of Chemistry,
Texas A&M University, College Station, Texas 77843

Study of *trans*-Dichlorobis(ethylenediamine)nickel(III) in Zeolite Y

HANFAN LIU, WENXIA SHEN, WILLIAM H. QUAYLE, and JACK H. LUNSFORD*

At temperatures as low as −40 °C [Ni^{II}(en)$_2$]$^{2+}$ (en = ethylenediamine) in zeolite Y is oxidized with molecular chlorine to a complex that contains nickel(III) in a low-spin state. The EPR spectrum indicates that the d^7 ion is in D_{4h} symmetry with two equivalent chlorine atoms along the symmetry axis. The paramagnetic species is attributed to the [Ni^{III}(en)$_2$Cl$_2$]$^+$ complex that is formed within the large cavities of the zeolite. At 25 °C this complex decays with a half-life of ca. 30 h.

Introduction

Intracrystalline cavities of zeolites provide an interesting environment for carrying out redox chemistry involving transition-metal ions. In previous work [Ru^{II}(bpy)$_3$]$^{2+}$ (bpy = bipyridine) in zeolite Y was oxidized with Cl$_2$ to the corresponding Ru(III) complex and reduced back to Ru(II) with water.[1] Although no O$_2$ was produced from the water, a small

amount of CO$_2$ was observed in which the oxygen was derived from the water. In the present study a nickel(III) complex has been formed, again by oxidation with molecular chlorine, and in this case the resulting chloride ions enter the first coordination sphere.

The chemistry of Ni(III) is described in two reviews.[2,3] A number of Ni(III) complexes have been reported in which the

(1) Quayle, W. H.; Lunsford, J. H. *Inorg. Chem.* **1982**, *21*, 97.

(2) Nag, K.; Chakravorty, A. *Coord. Chem. Rev.* **1980**, *33*, 87.
(3) Haines, R. I.; McAuley, A. *Coord. Chem. Rev.* **1981**, *39*, 77.

metal ion is coordinated to four or more nitrogen atoms.[4-9] The ligands include en, bpy, and cyclam (1,4,8,11-tetrazacyclotetradecane = L). In the presence of halide ions and cyclam Ni(II) may be oxidized to the *trans*-[Ni^{III}X$_2$L]$^+$ complex, where X = Cl$^-$ or Br$^-$.[4] This complex is similar in many respects to that which has been observed in the zeolite. The resulting low-spin Ni(III) complexes exhibit characteristic EPR spectra that provide electronic and structural information.

The formation of [Ni^{III}(en)$_2$]$^{3+}$ and [Ni^{III}(en)$_3$]$^{3+}$ complexes during pulse radiolysis of aqueous solutions has been followed with use of an absorption band at 300 nm.[6] In addition, Babaeva and co-workers[7] have synthesized pure compounds of the form [Ni^{III}(en)$_2$Cl$_2$]X, where X may be Cl$^-$ or ClO$_4^-$. These low-spin Ni(III) complexes were characterized by infrared spectroscopy and magnetic susceptibility measurements.[7,8]

Experimental Section

A bis(ethylenediamine)nickel(II) complex in water was prepared from stoichiometric amounts of ethylenediamine and Ni(NO$_3$)$_2$. A typical solution containing 0.0097 M Ni(II) and 0.0194 M en at pH 8.25 has 17% [Ni^{II}(en)]$^{2+}$, 68% [Ni^{II}(en)$_2$]$^{2+}$, and 15% [Ni^{II}(en)$_3$]$^{2+}$, as calculated from published equilibrium constants.[10] Aqueous suspensions of sodium–Y zeolite (Linde, lot no. Y-52-3365-94) containing 0.25 wt % solid were placed in a flask and equilibrated for 48 h at 25 °C with Ni(II)-en solutions. The pH of these solutions was 9.8–10. By variance of the concentration of Ni and en, zeolite samples with different nickel exchange levels were obtained. After the exchange step the zeolite samples were dried in air. The nickel content, as determined by atomic absorption spectrometry, was in the range 0.03–8.0 nickel ions/unit cell, which corresponds to 0.004–1.0 complex/large cavity. Nickel-61, obtained from Oak Ridge National Laboratory in the elemental form, was reacted with HNO$_3$ and then with en.

Nickel(III) complexes were formed by the chlorination of the zeolites. The zeolite samples were partially dehydrated by heating to 60 °C or higher temperatures for 4 h under a vacuum that ultimately was 10^{-5} torr. The chlorination reactions were carried out at different temperatures by exposing the samples to successive doses of chlorine or by maintaining a constant pressure of chlorine during the reaction. Excess chlorine was removed by evacuation prior to obtaining spectra.

Most of the EPR spectra were recorded with the sample at 77 K by using a Varian E-6S X-band spectrometer. The *g* values were determined relative to a phosphorous-doped silicon standard, with *g* = 1.9987, which was attached to the outside of the sample tube. Spin concentrations were calculated by numerical double integration of the derivative spectra and comparison of that with the double integral of the phosphorus-doped silicon standard of known spin concentration. Simulated EPR spectra were calculated by using the computer program SIM-13.[11]

Infrared spectra were recorded at room temperature with a Perkin-Elmer 580B spectrophotometer. The zeolite samples were in the form of self-supporting wafers having a mass per unit area of 4–6 mg/cm^2. The wafers were suspended in a Pyrex cell fitted with KCl windows. The samples were treated in situ with chlorine at −35 or 25 °C.

Diffuse-reflectance spectra were obtained with a Varian 2300 spectrophotometer with an integrating sphere. The zeolite samples (1.4 g) were prepared in one section of a cell and tapped into a fuzed-quartz cuvette. The data are reported as the logarithms of the Schuster–Kubelka–Munk remission function F(R_∞).[1]
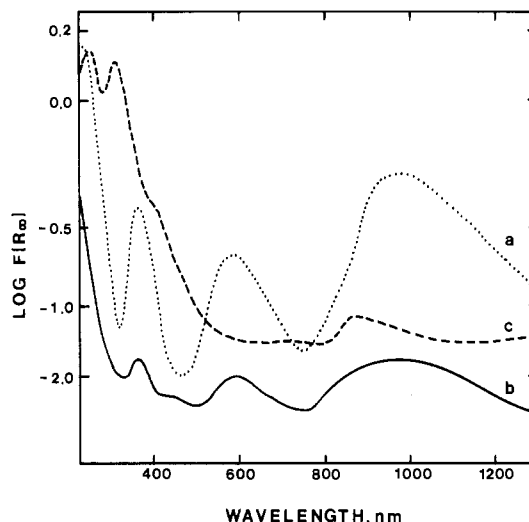
(4) Desideri, A.; Raynor, J. B.; Poon, C.-K. *J. Chem. Soc. Dalton Trans.* **1977**, 2051.
(5) Brodovitch, J. C.; Haines, R. I.; McAuley, A. *Can. J. Chem.* **1981**, *59*, 1610.
(6) Lati, J.; Meyerstein, D. *Inorg. Chem.* **1972**, *11*, 2397.
(7) Babaeva, A. V.; Baranovskii, I. B.; Afanaseva, G. G. *Russ. J. Inorg. Chem. (Engl. Transl.)* **1965**, *10*, 1268.
(8) Baranovskii, I. B.; Mazo, G. Ya. *Russ. J. Inorg. Chem. (Engl. Transl.)* **1975**, *20*, 444.
(9) Lappin, A. G.; Murray, C. K.; Margerum, D. W. *Inorg. Chem.* **1978**, *17*, 1630.
(10) Bjerrum, J., Ed. "Stability Constants"; The Chemical Society: London, 1957; Part I.
(11) Lozos, G.; Hoffman, B.; Franz, B. *QCPE* **1974**, *No. 265*.

Figure 1. Diffuse-reflectance spectra: (a) [Ni^{II}(en)$_2$]Cl$_2$·2H$_2$O; (b) [Ni^{II}(en)$_2$]–Y zeolite; (c) sample from (b) 20 min after addition of Cl$_2$.
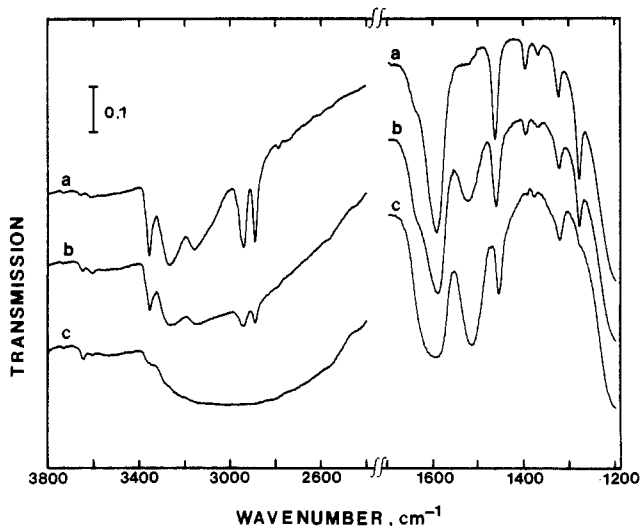

Figure 2. Infrared spectra of nickel complexes in zeolite Y: (a) [Ni^{II}(en)$_2$]–Y zeolite; (b) sample from (a) after addition of Cl$_2$ (Cl$_2$/Ni = 3.5); (c) sample from (b) after addition of excess Cl$_2$ at 25 °C.

The XPS spectra were obtained with a Hewlett-Packard 5950A spectrometer with Al Kα X rays (1486.6 eV). The atomic ratios were calculated from the equation $\eta_1/\eta_2 = (I_1/I_2)(\sigma_2/\sigma_1)$, where the peak area, *I*, was normalized to the same number of scans, and the photoionization cross sections reported by Scofield[12] were used.

Results and Discussion

Identification of [Ni^{II}(en)$_2$]$^{2+}$ Complexes in Zeolite Y. The exchange of ethylenediamine complexes in Y-type zeolites previously has been demonstrated with the use of [Cu^{II}(en)$_2$]$^{2+}$, and more recent work has shown that the analogous nickel(II) complex may be exchanged into montmorillonite clays.[13,14] In Figure 1a,b the diffuse-reflectance spectra of [Ni^{II}(en)$_2$]-Cl$_2$·2H$_2$O and a zeolite ion exchanged with predominantly [Ni^{II}(en)$_2$]$^{2+}$ complexes to a level of 8 Ni ions/unit cell are compared. Spectrum a exhibits absorbance maxima at 362, 585, and 975 nm, which may be compared with maxima at 362, 590, and 980 nm for spectrum b. Within experimental error the absorption maxima are the same, which provides

(12) Scofield, J. H. *J. Electron Spectrosc. Relat. Phenom.* **1976**, *8*, 129.
(13) Peigneur, P.; Lunsford, J. H.; DeWilde, W.; Schoonheydt, R. A. *J. Phys. Chem.* **1977**, *81*, 1179.
(14) Schoonheydt, R. A.; Velghe, F.; Uytterhoeven, J. B. *Inorg. Chem.* **1979**, *18*, 1842.

Table I. Superficial and Bulk Atomic Ratios for a [Ni^{II}(en)$_2$]–Y Zeolite

	atomic ratios		
	Si/Al	Ni/Si	Ni/Al
surface	2.96	0.017	0.051
bulk	2.47	0.042	0.101

convincing evidence that the principal complex in the zeolite was indeed [Ni^{II}(en)$_2$]$^{2+}$. By comparison the [Ni^{II}(en)]$^{2+}$ spectrum is red shifted 10–40 nm and the [Ni^{II}(en)$_3$]$^{2+}$ spectrum is blue shifted 20–50 nm relative to the spectrum of the [Ni^{II}(en)$_2$]$^{2+}$ complex in aqueous solution.

The infrared spectrum of the [Ni^{II}(en)$_2$]$^{2+}$ complex in zeolite Y, depicted in Figure 2a, also is in good agreement with that reported for the [Ni^{II}(en)$_2$]Cl$_2$ compound.[8] Minor differences occur in the positions due to the NH$_2$ stretch at 3300 and 3335 cm^{-1}. In the zeolite these bands appear at 3270 and 3360 cm^{-1}. The shift in the zeolite may be due to hydrogen bonding between the en ligand and the oxygens of the zeolite lattice. The shoulder at 1640 cm^{-1} is due to zeolitic water that was not removed by the dehydration procedure. Other small differences appear in the 1280–1465-cm^{-1} region of the spectrum.

The location of the complex, either on the external surface of the zeolite crystallite or within the zeolite cavities, also was of interest. Previously, XPS has been effectively used to distinguish between these two locations.[15] Since the escape depth of electrons is 20–40 Å, only ions near the surface of a zeolite particle are detected. If enrichment of a Ni ion were to occur in this surface region, then the Ni/Si or Ni/Al ratios would be larger than those determined from a bulk analysis. The results of Table I clearly show that the near-surface Ni/Si and Ni/Al ratios are substantially less than the corresponding bulk ratios; thus it appears that the surface is somewhat depleted in [Ni^{II}(en)$_2$]$^{2+}$ complexes.

Formation of [Ni^{III}(en)$_2$Cl$_2$]$^+$ Complexes. No EPR signal could be detected for the [Ni^{II}(en)$_2$]–Y samples; however, upon addition of Cl$_2$ to the zeolite the spectrum shown in Figure 3a was observed. This particular sample contained 0.27 Ni ion/unit cell. The spectrum is characteristic of a low-spin d^7 ion in axial symmetry ($g_\perp > g_\parallel \simeq 2.0$). The magnetic parameters are summarized in Table II and compared with the values reported for [Ni^{III}(cyclam)Cl$_2$]$^+$.[4] The seven-line hyperfine spectrum, centered on the field corresponding to $g_\parallel$, is consistent with two trans chlorine atoms ($I = {}^3/_2$) interacting with an unpaired electron which is primarily in a d$_{z^2}$ orbital. The hyperfine splitting of $A_\parallel{}^{Cl} = 29$ G is in good agreement with the value of 28 G for [Ni^{III}(cyclam)Cl$_2$]$^+$ as reported by Desideri et al.[4] The hyperfine splitting in the perpendicular direction is not resolved; however, from the width of the line one may conclude that $A_\perp{}^{Cl} = 8 \pm 2$ G. Assuming 8 G as the correct value, the chlorine 3s and 3p character for each chlorine is ca. 0.9 and 14%, respectively. Here, the hyperfine splitting for an unpaired electron in a pure 3s and 3p orbital on chlorine is taken to be 1617 and 98 G, respectively.[4]

The EPR spectrum of the corresponding ^{61}Ni(III) ($I = {}^3/_2$) complex is shown in Figure 3b. In this spectrum each chlorine hyperfine line is split into four lines; the outer lines can only be detected at higher amplification (Figure 3c). The simulated spectrum was rather insensitive to $A_\perp{}^{Ni}$, although a value of 6 ± 4 G gave a good fit to the experimental spectrum.

For a low-spin d^7 ion in D_{4h} symmetry, the hyperfine coupling constants are given by

$$A_\perp{}^{Ni} = A_{iso}{}^{Ni} - B^{Ni}(1 - (45/12)\Delta g_\perp) \quad (1)$$

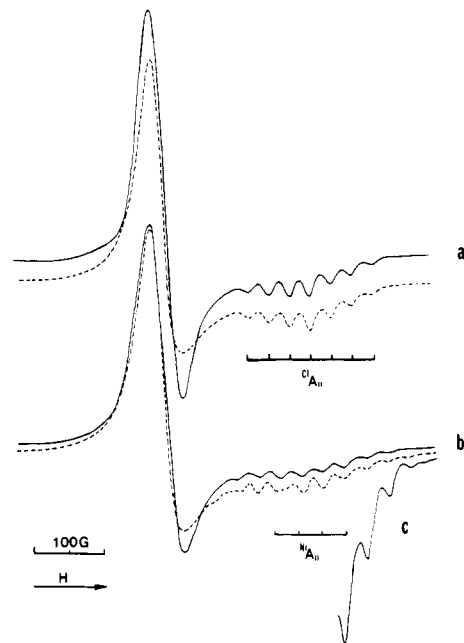$$A_\parallel{}^{Ni} = A_{iso}{}^{Ni} + 2B^{Ni}(1 - \Delta g_\perp/4) \quad (2)$$

(15) Pedersen, L. A.; Lunsford, J. H. *J. Catal.* **1980**, *61*, 39.

Figure 3. EPR spectra of [Ni^{III}(en)$_2$Cl$_2$]$^+$ complex in zeolite Y: (a) ^{60}Ni(III) complex; (b) ^{61}Ni(III) complex; (c) ×10 amplification of spectrum b. Solid lines are the experimental spectra; dashed lines are the simulated spectra.

where $A_{iso}{}^{Ni}$ and B^{Ni} are the isotropic and anisotropic hyperfine parameters in the absence of orbital magnetism and $\Delta g_\perp = g_\perp - g_e$. The sign of a B^{Ni}, and therefore $A_\parallel{}^{Ni}$, must be positive for an unpaired electron in a d$_{z^2}$ orbital, but the sign of $A_\perp{}^{Ni}$ is not known. If one assumes a negative sign, then $A_{iso}{}^{Ni} = -65$ G and $2B^{Ni} = 33$ G. With use of $2B^{Ni} = 75.5$ G for an electron entirely in a 3d orbital,[16] the deduced 3d character is 43%. The 4s character is more difficult to calculate because of spin-polarization effects, but values are typically less than 10%.[17] Thus, within these approximations and the sign choice the total spin density on the two chlorines and the nickel atom is ca. 70%.

We have prepared [Ni^{III}(en)$_2$Cl$_2$]Cl·HCl·2H$_2$O according to the method of Babaeva et al.[7] and have observed the EPR spectrum of this complex. The g values shown in Table II are in reasonably good agreement with those reported by Yamashita et al.[18] and with the values observed for the [Ni^{III}(en)$_2$Cl$_2$]$^+$ complex in zeolite Y. In the nominally pure material approximately 70% of the Ni could be accounted for in the EPR spectrum, which substantiates that one is actually observing by EPR the spectrum of the [Ni^{III}(en)$_2$Cl$_2$]$^+$ complex, rather than some minor component.

The location of the paramagnetic complex also was of interest, and to determine the location, a paramagnetic molecule that was too large to go into the cavities was added to a slurry containing the zeolite. Nickel complexes on the external surfaces would experience spin–spin broadening, whereas those in the cavities would not be affected. In this experiment a partially degassed zeolite containing 0.64 Ni ion/unit cell was oxidized with Cl$_2$ and then slurried in oxygen-free benzene. In the presence of benzene the spin intensity increased about 25% and did not change after 24 h (see below). The benzene was removed under vacuum, and a 0.1 M solution of 2,2′-diphenyl-1-picrylhydrazyl (DPPH) in benzene was added to the sample. It was observed that the Ni(III) spin concentration decreased 12% relative to the sample that contained pure

(16) Goodman, B. A.; Raynor, J. B. *Adv. Inorg. Chem. Radiochem.* **1970**, *13*, 135.

(17) Symons, M. C. R.; Wilkinson, J. G. *J. Chem. Soc. A* **1971**, 2069.

(18) Yamashita, M.; Nonaka, Y.; Kida, S. *Inorg. Chim. Acta* **1981**, *52*, 43.

Table II. EPR Parameters for Ni(III) Complexes

complex	$g_\parallel$	$g_\perp$	$A_\parallel^{Cl}$, G	$A_\perp^{Cl}$, G	$A_\parallel^{61Ni}$, G	$A_\perp^{61Ni}$, G
[Ni^{III}(en)$_2$Cl$_2$]Y	2.010	2.154	29	8 ± 2	33	6 ± 4
[Ni^{III}(en)$_2$Cl$_2$]Cl·HCl·2H$_2$O^a	2.019	2.184				
[Ni^{III}(en)$_2$Cl$_2$]Cl^b	2.020	2.20				
[Ni^{III}(en)$_2$Cl$_2$]Cl/MeOH^c	2.017	2.160	29.5	8 ± 2		
[Ni^{III}(cyclam)$_2$Cl$_2$]ClO$_4$^{d}	2.022	2.180	28	<5		

^{a} Compound diluted by mixing with KCl. ^{b} Reference 18. ^{c} Complex slightly soluble in methanol. ^{d} Reference 4.
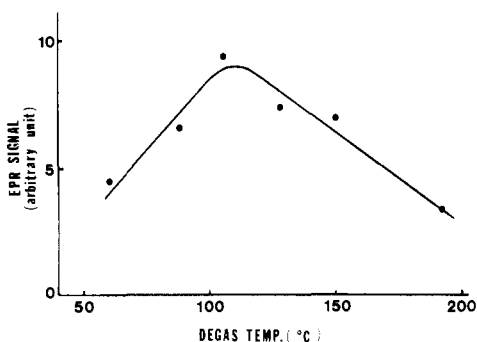

Figure 4. Effect of degassing temperature on the [Ni^{III}(en)$_2$Cl$_2$]$^+$ concentration.

benzene. We conclude, therefore, that only about 10% of the [Ni^{III}(en)$_2$Cl$_2$]$^+$ was on or near the external surface.

The formation of [Ni^{III}(en)$_2$Cl$_2$]$^+$ in zeolite Y is further supported by the diffuse-reflectance spectrum of Figure 1c. Upon addition of Cl$_2$ to the sample containing 8 Ni ions/unit cell the spectrum of the [Ni^{II}(en)$_2$]$^{2+}$ complex disappeared and new bands were observed at 255, 315, and 875 nm. In a separate study carried out in aqueous HCl solution, we have demonstrated that the band at 315 nm is associated with the EPR spectrum of the [Ni^{II}(en)$_2$Cl$_2$]$^+$ complex.[19] Moreover, from the study of nickel–amine complexes in aqueous solution it is apparent that the ratio of molar extinction coefficients for the λ = 315 nm band of [Ni^{III}(en)$_2$Cl$_2$]$^+$ and the λ = 362 nm band of [Ni^{II}(en)$_2$]$^{2+}$ exceeds 400. Thus, although the band at 315 nm in Figure 1c is large, it represents only a small fraction of the nickel in the zeolite (see below).

Variation in Ni(III) Concentration. The Ni(III) concentration, as determined by EPR, depended upon such factors as the nickel loading, the degassing temperature, the temperature of chlorination, the manner in which the chlorine was added, and the time after chlorination. As determined by EPR, a maximum net conversion of 15% of the Ni(II) into Ni(III) was achieved with a sample having 0.3 Ni ion/unit cell after degassing at 100 °C and chlorination at –30 °C for 20 min. The Ni(III) complex in this sample had a half-life at 25 °C of 32 h with zero-order decay kinetics. As shown in Figure 4, the concentration of the Ni(III) species reached a maximum for samples that had been dehydrated at 110 °C. The formation of Ni(III) complexes was not affected by light, in either the visible or the ultraviolet region of the spectrum.

The Ni(III) spin concentration also was a function of the manner in which Cl$_2$ was dosed onto the sample. The addition of small Cl$_2$ doses (Cl$_2$/Ni = 0.15) at 25 °C resulted in maximum spin concentrations. With use of this technique a maximum spin concentration was achieved at a total ratio of Cl$_2$/Ni ≃ 3. Thereafter the spin concentration remained constant. For samples that contained 0.64 and 8.0 Ni ions/unit cell, 18% and 6%, respectively, of the Ni was detected as [Ni^{III}(en)$_2$Cl$_2$]$^+$ by EPR. When the same amount of Cl$_2$ was added at one time, the observed Ni(III) was about one-fourth as great.

The addition of Cl$_2$ had a marked effect on the infrared spectra of the ligands as shown in Figure 2b,c. The zeolite described here contained 8.0 Ni ions/unit cell. Upon addition of the Cl$_2$ in small doses, the bands in the 3000-cm^{-1} region broadened greatly, the bands at 1280 and 1400 cm^{-1} decreased, the band at 1595 cm^{-1} broadened, and a strong new band appeared at 1520 cm^{-1}. Although the identity of the new species is not certain, it is evident that many of the en ligands reacted with chlorine and that [Ni^{III}(en)$_2$Cl$_2$]$^+$ was not a dominant complex in the sample, which is in agreement with the EPR and diffuse-reflectance results.

The formation and further reaction of [Ni^{III}(en)$_2$Cl$_2$]$^+$ obviously are complex processes, and water is believed to be a factor in both steps. The oxidation of Ni(II) to Ni(III) involves a one-electron transfer, yet two chloride ions are present in the complex. It is reasonable to expect that at least one of the chloride ions is formed by the reaction

$$Cl_2 + 20H^- \rightarrow Cl^- + ClO^- + H_2O \qquad (3)$$
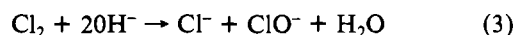
The slow decay of the Ni(III) complex is not surprising in view of the observation by Babaeva et al.[7] that the [Ni^{III}(en)$_2$Cl$_2$]$^+$ complex is unstable in water.

We have confirmed this observation and have found that the complex reacts much more slowly in a solution of HCl and H$_2$O at pH 0.5.[19] These results support the suggestion by Lati and Meyerstein[6] that the reaction

$$[Ni^{III}(en)_n]^{3+} + OH^- \rightarrow [Ni^{II}(en)_n]^{2+} + OH\cdot \qquad (4)$$

may, in part, be responsible for the reduction of Ni(III) in their pulse radiolysis experiments. We propose that the long-term loss of Ni(III) results from its reaction with hydroxide ions. The zero-order kinetics indicates that the reaction rate may be limited by the diffusion of OH$^-$ in the zeolite. When benzene is adsorbed in the zeolite, reaction 4 may be impeded.

The increase in Ni(III) concentration with increasing dehydration temperature, up to 110 °C, lends support to the role of water in the destruction of the [Ni^{III}(en)$_2$Cl$_2$]$^+$ complex. The maximum concentration at 110 °C, shown in Figure 4, may occur because of the instability of the nickel–ligand bonds at higher temperatures. Schoonheydt et al.[14] have noted that the [Ni^{II}(en)$_2$]^2 complex is unstable in the montmorillonite at 200 °C, and there is evidence that the complex is less stable in zeolites.[20]

The mechanism for the reaction of the ligands at higher Cl$_2$ concentrations is unclear; however, the strong infrared bands at 1520 and 1600 cm^{-1} in Figure 2c are consistent with the formation of amine hydrochloride molecules.[21]

(19) Shen, W.; Lunsford, J. H., unpublished results.

(20) Peigneur, P. Ph.D. Dissertation, University of Leuven, Leuven, Belgium, 1976.

(21) Alpert, N. L.; Keiser, W. E.; Szymanski, H. A. "Theory and Practice of Infrared Spectroscopy"; Plenum Press: New York, 1973; p 281.